

The hydrogeologic framework sets the lithologic constraints through which water is likely to flow. This framework is based on direct outcrop observations (Figure 2-20), geologic observations from boreholes in the area, interpolation from the regional hydrogeology, geophysical logs (especially resistivity and seismic surveys), and geologic inferences of lithologic unit thicknesses from regional facies variations. Representative cross sections of the site-scale hydrogeologic framework model are presented in Figure 2-21.

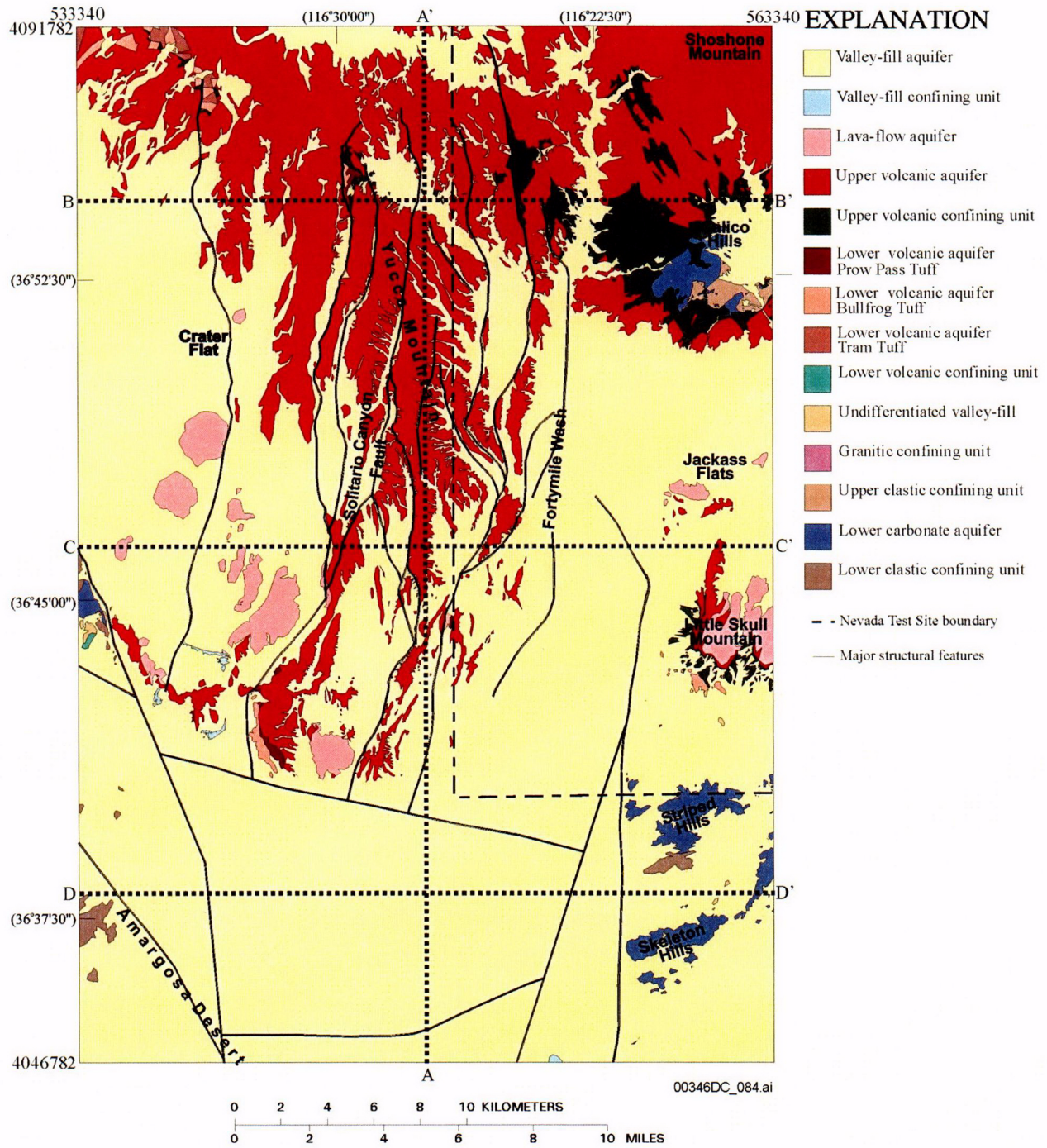
Aspects of the site-scale geology important to groundwater flow are represented in the site-scale hydrogeologic framework model. A detailed description of the hydrogeologic framework model, assumptions, and methods used to develop the model are given in *Hydrogeologic Framework Model for the Saturated-Zone Site-Scale Flow and Transport Model* (USGS 2001c). A comparison of the revised hydrogeologic framework model with the geologic framework model used to evaluate the detailed site geology is presented in Appendix A.

Since development of the hydrogeologic framework model used in the total system performance assessment license application base-case model, the Yucca Mountain hydrogeologic framework model has been reinterpreted incorporating data recently obtained from the Nye County Early Warning Drilling Program and through the reinterpretation of existing data from other areas (including geophysical data in the northern area of the site). The major changes in the revised hydrogeologic framework model are in the southern part of the model and include new information on the depths and extent of the alluvial layers.

As a result of reinterpreting the hydrogeologic framework model, the number and distribution of hydrogeologic units has been modified in the 2002 hydrogeologic framework model, and it now corresponds to the units in the regional hydrogeologic framework model. A comparison of the hydrogeologic units identified in the hydrogeologic framework models used in the base-case and 2002 models is provided in Table 2-6. The table indicates that there were 19 hydrogeologic units in the base-case hydrogeologic framework model and 27 hydrogeologic units in the 2002 hydrogeologic framework model. Four of the 27 units present in the regional model are not found within the boundary of the site-scale hydrogeologic framework model because they are pinched out by adjacent units. The hydrogeologic framework model revision has the same units and is consistent with the Death Valley regional flow system model (D'Agnese et al. 2002).

The development of the 2002 site-scale hydrogeologic framework model revision was influenced primarily by geologic observations made from Nye County boreholes drilled since the earlier version of the model. Although these boreholes serve multiple geologic and hydrogeologic purposes, an important use has been to better characterize the thickness and lateral extent of the alluvial aquifer north of U.S. Highway 95. The location of these Nye County boreholes and cross-section lines are illustrated in Figure 2-22.

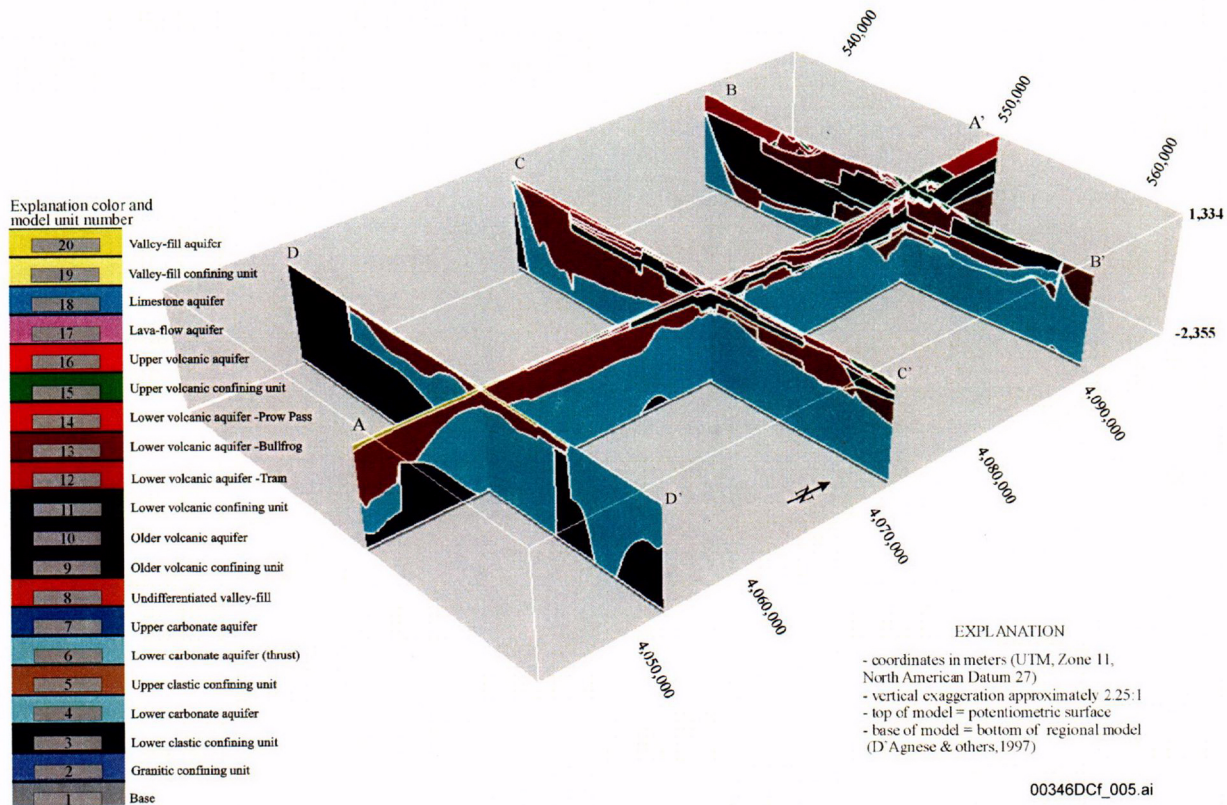
Figure 2-23 shows the cross-sections for these Nye County boreholes. Figures 2-24 and 2-25 depict the total alluvial thickness and saturated alluvial thickness derived from borehole observations and geophysical logging completed in the area between Yucca Mountain and U.S. Highway 95.



Source: USGS 2001c, Figure 4-2.

NOTE: The lines of section correspond to the cross sections shown on Figure 2-21.

Figure 2-20. Outcrop Geology of the Site-Scale Hydrogeologic Framework Model



Source: USGS 2001c, Figure 6-1.

Note: "D'Agnese & others, 1997" refers to D'Agnese et al. (1997).

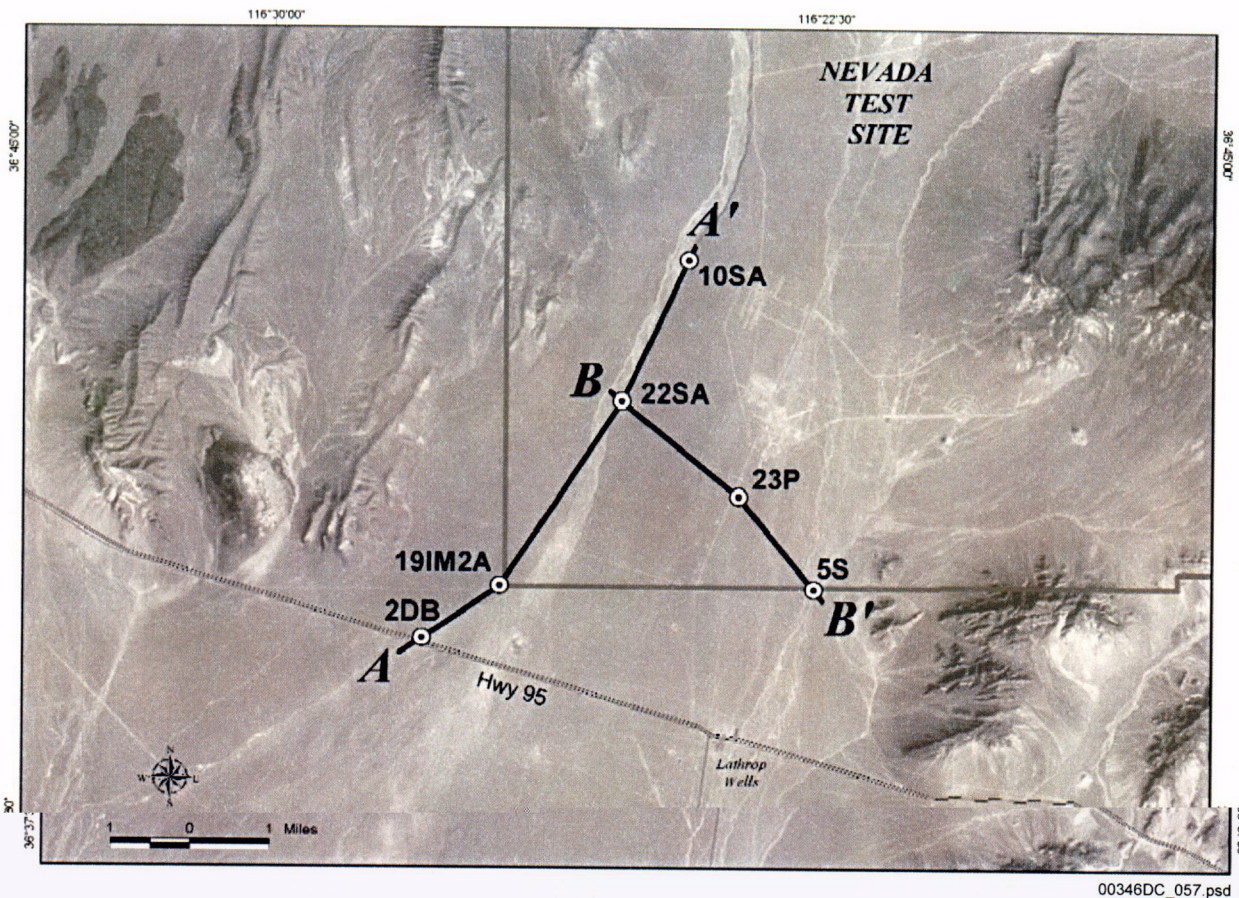
Figure 2-21. Representative Cross-Sections through the Site-Scale Hydrogeologic Framework Model

Table 2-6. Correspondence between Units of the Revised- and Base-Case Hydrogeologic Framework Models

Abbreviation	Revised (Site and Regional Transient Model in Preparation)		Base-Case Hydrogeologic Framework Model	
	Hydrogeologic Name	Unit	Unit	Hydrogeologic Name
Base	Base (-4000 m)	1	1	Base (bottom of regional flow model)
ICU	Intrusive Confining Unit	2	2	Granitic confining unit (granites)
XCU	Crystalline Confining Unit	3	3	Lower Clastic Confining Unit (lccu)
LCCU	Lower Clastic Confining Unit	4	3	Lower Clastic Confining Unit (lccu)
LCA	Lower Carbonate Aquifer	5	4	Lower Carbonate Aquifer (lca)
UCCU	Upper Clastic Confining Unit	6	5	Upper Clastic Confining Unit, Upper Clastic Confining Unit—thrust 2 (uccu, uccut2)
UCA	Upper Carbonate Aquifer	7	NA	NA
LCCU_T1	Lower Clastic Confining Unit—thrust	8	NA	Lower Clastic Confining Unit—thrust 1 (lccut1)
LCA_T1	Lower Carbonate Aquifer—thrust	9	6	Lower Carbonate Aquifer thrusts 1 and 2 (lcat1, lcat2)
SCU	Sedimentary Confining Unit (none in site area)	NA	NA	NA
VSU Lower	Lower Volcanic and Sedimentary Units	11	8	Undifferentiated valley-fill (leaky)
OVU	Older Volcanic Units	12	9, 10, 11	Older Volcanic Confining Unit, Older Volcanic Aquifer, Lower Volcanic Confining Unit (lvcu, lva, mvcu)
BRU	Belted Range Unit (none in site area)	NA	NA	NA
CFTA	Crater Flat - Tram Aquifer	14	12	Lower Volcanic Aquifer—Tram Tuff (tct)
CFBCU	Crater Flat - Bullfrog Confining Unit	15	13	Lower Volcanic Aquifer—Bullfrog Tuff (tcb)
CFPPA	Crater Flat - Prow Pass Aquifer	16	14	Lower Volcanic Aquifer—Prow Pass Tuff (tcp)
WVU	Wahmonie Volcanic Unit	17	15	Upper Volcanic Confining Unit (uvcu)
CHVU	Calico Hills Volcanic Unit	18	15	Upper Volcanic Confining Unit (uvcu)
PVA	Paintbrush Volcanic Aquifer	19	16	Upper Volcanic Aquifer (uva)
TMVA	Timber Mountain Volcanic Aquifer	20	16	Upper Volcanic Aquifer (uva)
VSU	Volcanic and Sedimentary Units	21	8	Undifferentiated valley-fill (leaky)
YVU	Young Volcanic Units (none in site area)	NA	NA	NA
LFU	Lavaflow Unit	23	17	Lava-flow Aquifer (basalts)
LA	Limestone Aquifer	24	18	Limestone Aquifer (amarts)
OACU	Older Alluvial Confining Unit (none in site area)	NA	NA	NA
OAA	Older Alluvial Aquifer	26	20	Valley-fill Aquifer (alluvium), Undifferentiated valley-fill (leaky)
YACU	Young Alluvial Confining Unit	27	19	Valley-fill Confining Unit (playas)
YAA	Young Alluvial Aquifer	28	20	Valley-fill Aquifer (alluvium)

Source: BSC 2003h, Table 7.5-2.

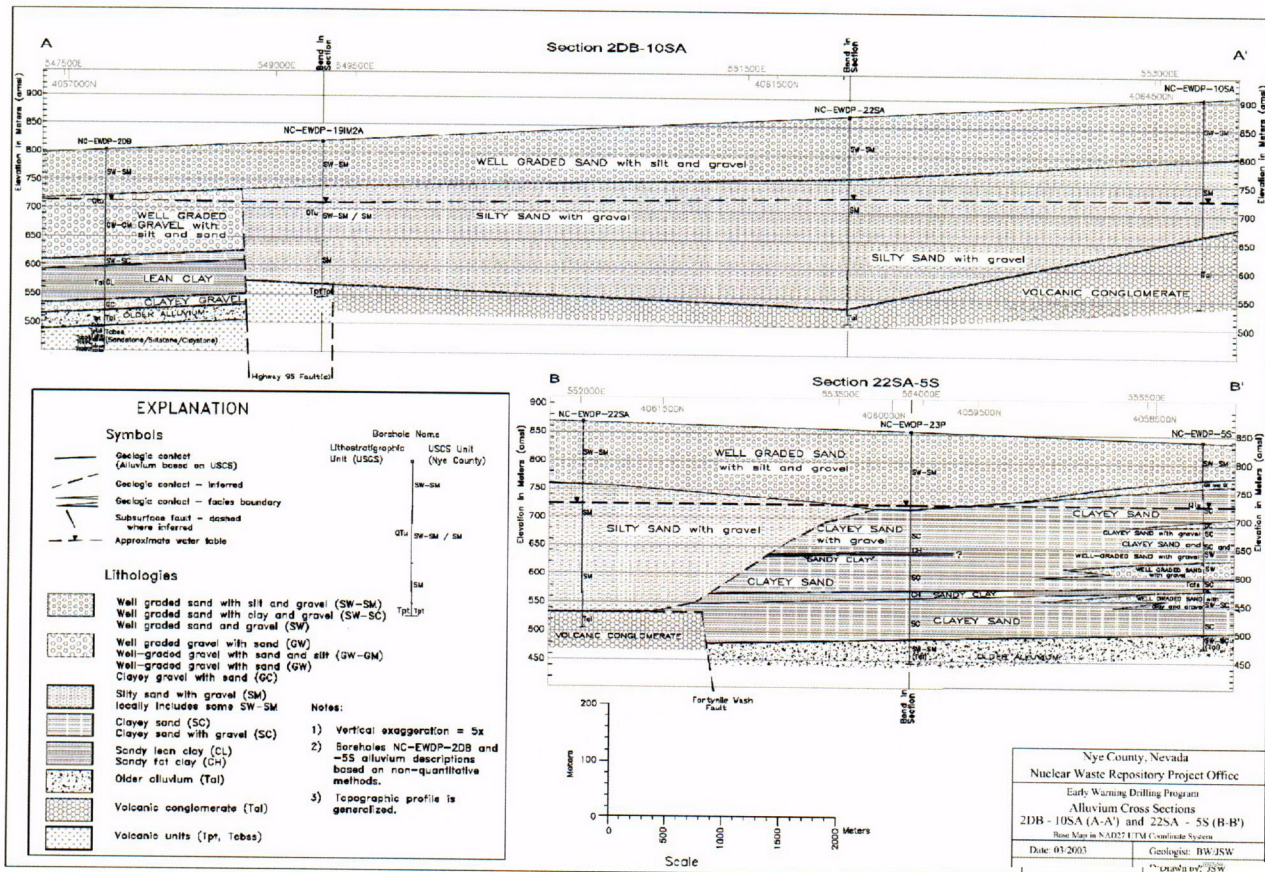
NOTE: These units do not have a one-to-one correlation. This table approximately relates the new hydrogeologic units to the base-case version. Four units that do not occur in the site-scale hydrogeologic framework model (OACU, YVU, BRU, and SCU) are included here to maintain the relationship to the regional model.



Source: Nye County Department of Natural Resources and Federal Facilities 2003, Figure 4.5-3.

NOTE: The cross sections A-A' and B-B' are shown in Figure 2-23.

Figure 2-22. Locations of Nye County Alluvium Cross Sections

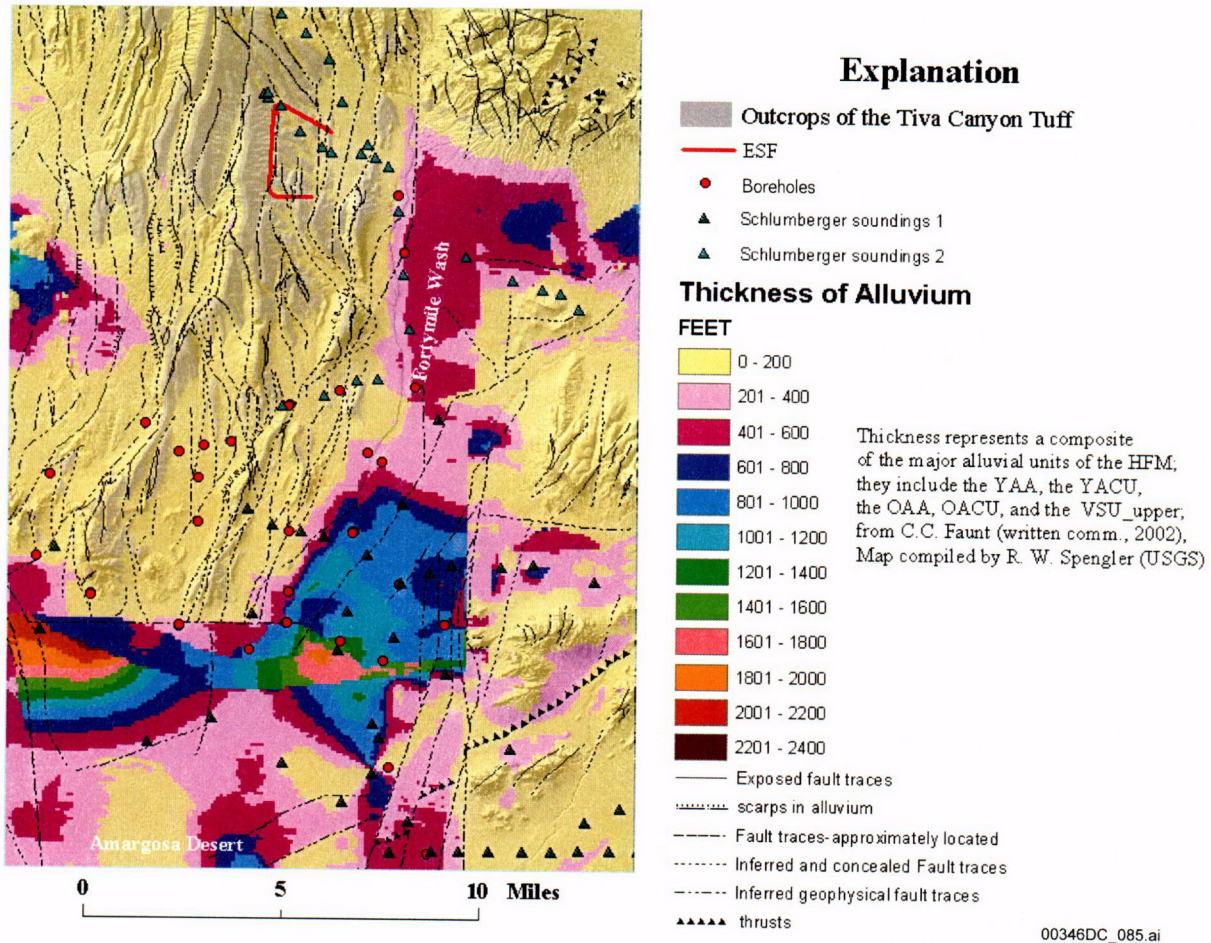


NOTES: USCS = Unified Soil Classification System; USGS = U.S. Geological Survey

00346DC_059.psd

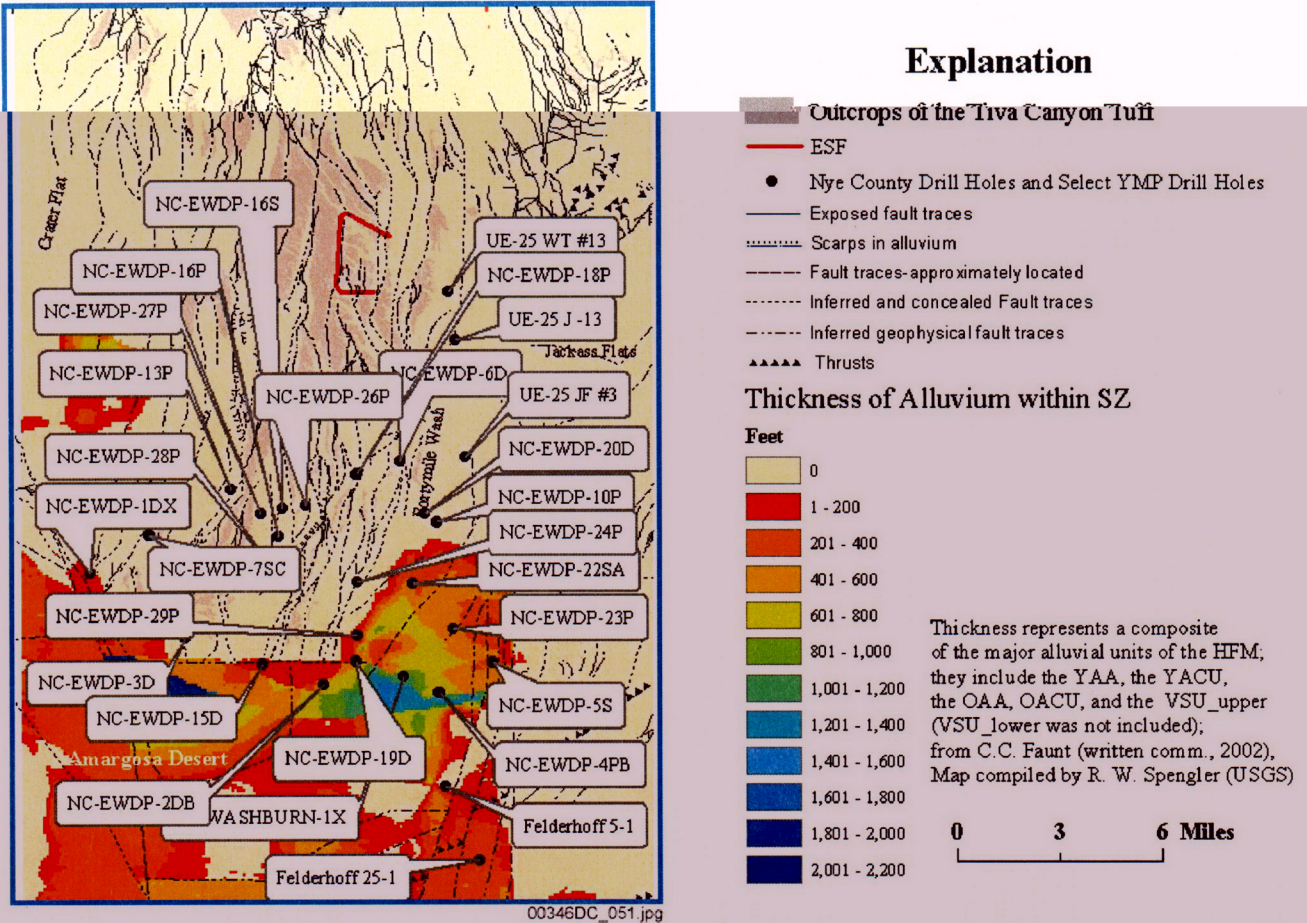
Source: Nye County Department of Natural Resources and Federal Facilities 2003, Figure 4.5-4.

Figure 2-23. Nye County Alluvium Cross Sections



Source: DTN: GS021008312332.002.

Figure 2-24. Alluvial Zone Total Thickness in the Vicinity of Yucca Mountain



Source: DTN: GS021008312332.002.

Figure 2-25. Alluvial Zone Saturated Thickness in the Vicinity of Yucca Mountain

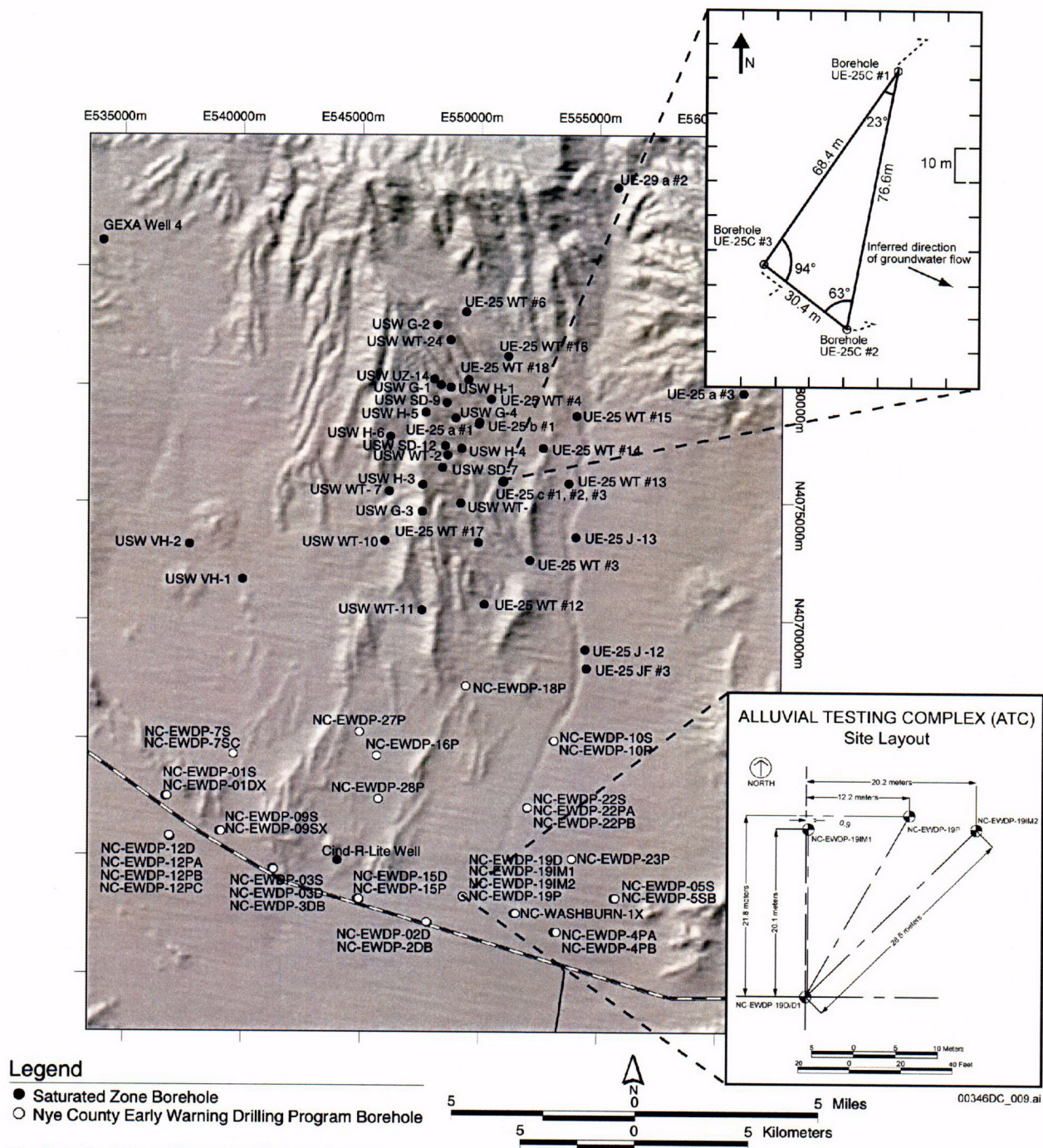
2.3.5 Site-Scale Hydrogeology

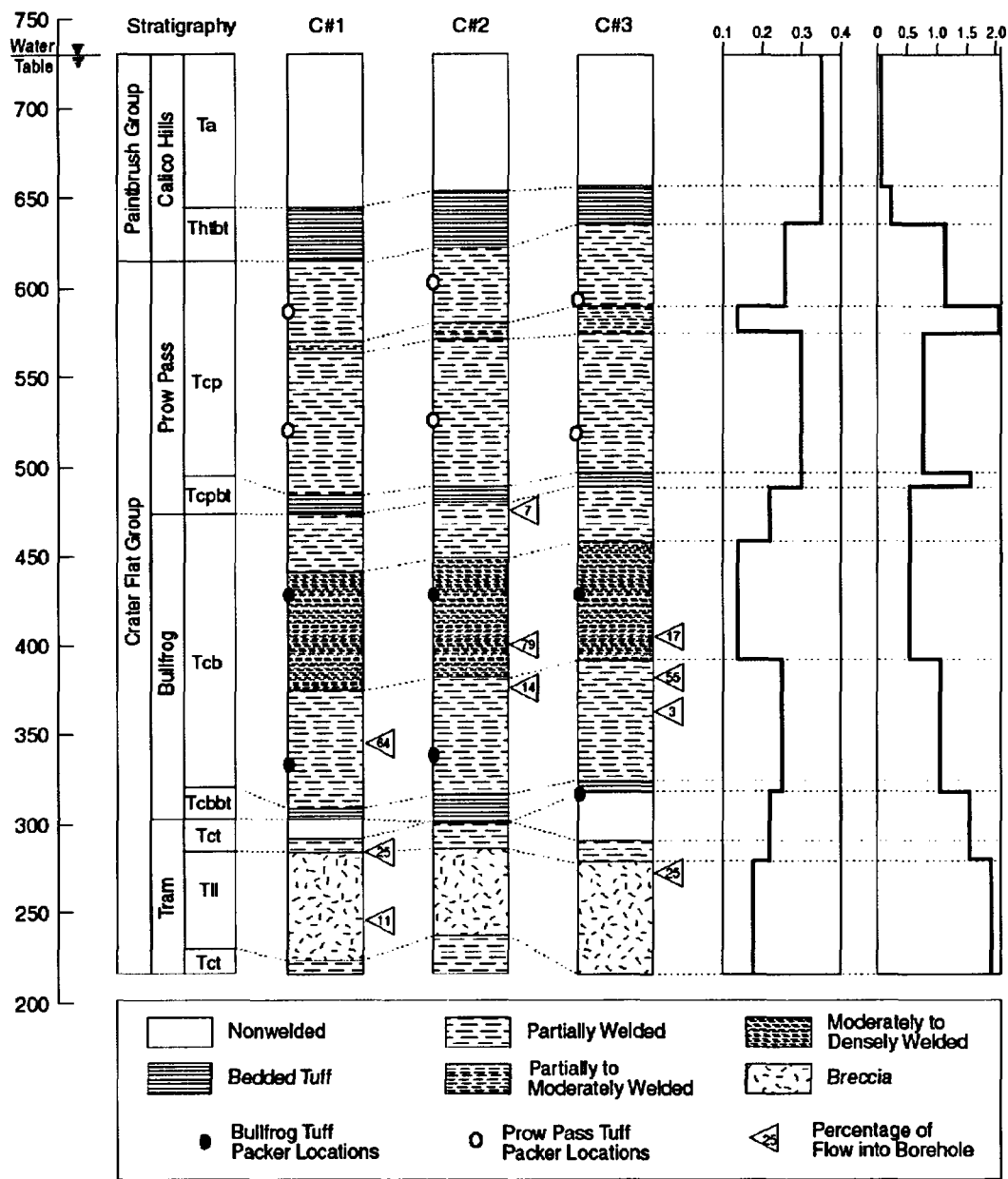
2.3.5.1 Site-Scale Hydrogeologic Characteristics

The permeability of rock units in the vicinity of Yucca Mountain has been determined by single and cross-hole hydraulic testing. These data have been used as starting points to support the calibration of the site-scale flow model (Section 2.3.7).

2.3.5.2 Tuff Hydrogeologic Characteristics Derived from Testing at the C-Wells

The C-Wells complex comprises three boreholes drilled and packed off in the Crater Flat Group. This complex is located about 700 m southeast of the South Portal of the Exploratory Study Facility (Figure 2-26), and it has been used to test the hydraulic and transport characteristics of the tuff aquifers along the likely travel path of groundwater from Yucca Mountain. Figure 2-27 summarizes the borehole construction and identifies the major flowing intervals observed in these three boreholes.





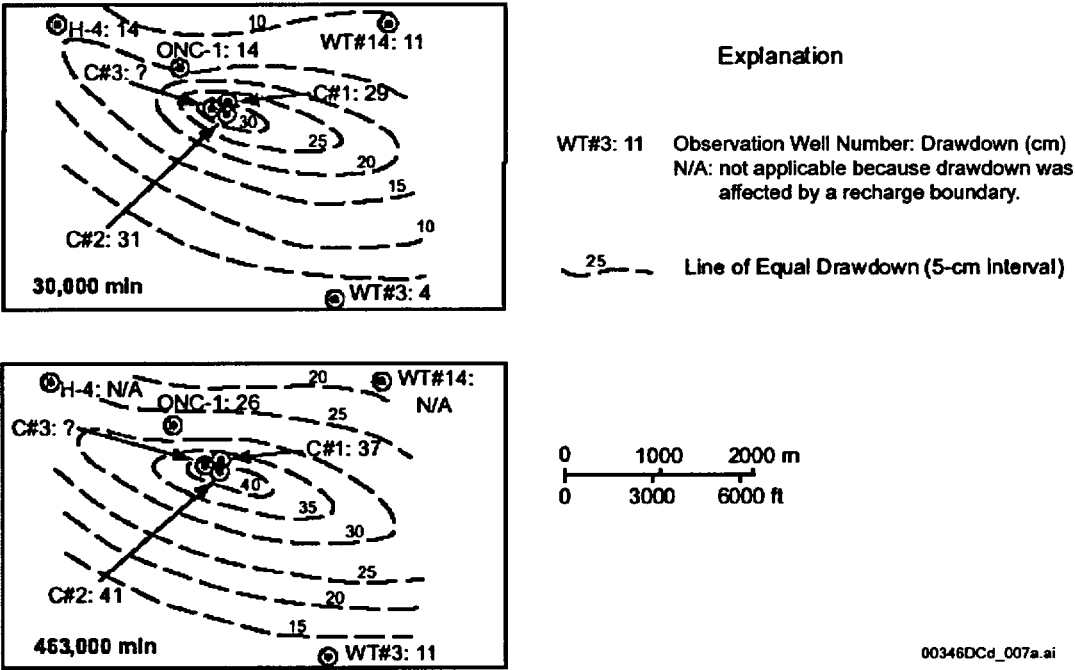
00346DC_050.jpg

Source. BSC 2003e, Figure 6.1-2.

NOTE: Packer locations indicate intervals in which tracer tests were conducted (tracer tests conducted between UE-25 c#2 and UE-25 c#3). The two borehole logs represent matrix porosity (dimensionless) and fracture density (number of fractures per meter), from left to right, respectively.

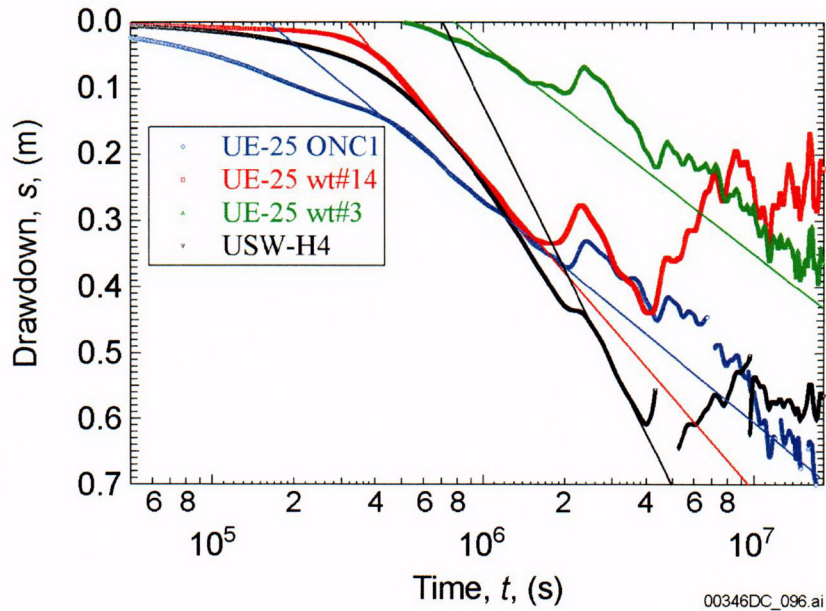
Figure 2-27. Stratigraphy, Lithology, Matrix Porosity, Fracture Density, and Inflow from Open-Hole Surveys at the C-Wells

In addition to the single- and cross-hole testing performed at the C-Wells, a large-scale pump test was performed in this complex. This test was conducted for more than a year and resulted in discernible drawdowns in boreholes located several kilometers away (Figures 2-28 and 2-29). These drawdowns indicate the lateral continuity of the saturated zone aquifer in these tuff rock units as well as similarities in transmissivities and average hydraulic characteristics.



Source: BSC 2003e, Figure 6.2-36.

Figure 2-28. Distribution of Drawdown in Observation Boreholes at Two Times After Pumping Started in UE-25 c#3



Source: BSC 2003e, Figure 6.2-39.

Figure 2-29. Drawdowns Observed in Boreholes Adjacent to the C-Wells Complex During the Long Term Pumping Test

2.3.5.3 Site-Scale Permeability Anisotropy

Anisotropic conditions exist if the permeability of media varies as a function of direction. Because groundwater primarily flows in fractures within the volcanic units downgradient of Yucca Mountain, and because fractures and faults occur in preferred orientations, it is possible that anisotropic conditions of horizontal permeability exist along the potential pathway of radionuclide migration in the saturated zone (BSC 2003e, Section 6.2.6). Performance of the repository could be affected by horizontal anisotropy if the permeability tensor is oriented in a north-south direction because the groundwater flow could be diverted to the south, causing any transported solutes to remain in the fractured volcanic tuff for longer distances before moving into the valley-fill alluvial aquifer (Figures 2-24 and 2-25). More southerly oriented flow directions would, therefore, reduce the length of the travel path through the alluvium to the compliance point. A reduction in the length of the flow path in the alluvium would decrease the amount of radionuclide retardation that could occur for radionuclides with greater sorption capacity in the alluvium than in fractured volcanic rock matrix. In addition, potentially limited matrix diffusion in the fractured volcanic units could lead to shorter transport times in the volcanic units relative to the alluvium.

A conceptual model incorporating horizontal anisotropy in the tuff aquifer is acceptable, given that flow in the tuff aquifer generally occurs in a fracture network that exhibits a preferential north-south strike azimuth. Major faults near Yucca Mountain that have been mapped at the surface and that have been included in the site-scale hydrogeologic framework model also have a similar preferential orientation (Figure 2-20). In addition, north to north-northeast striking structural features are optimally oriented perpendicular to the direction of least principal

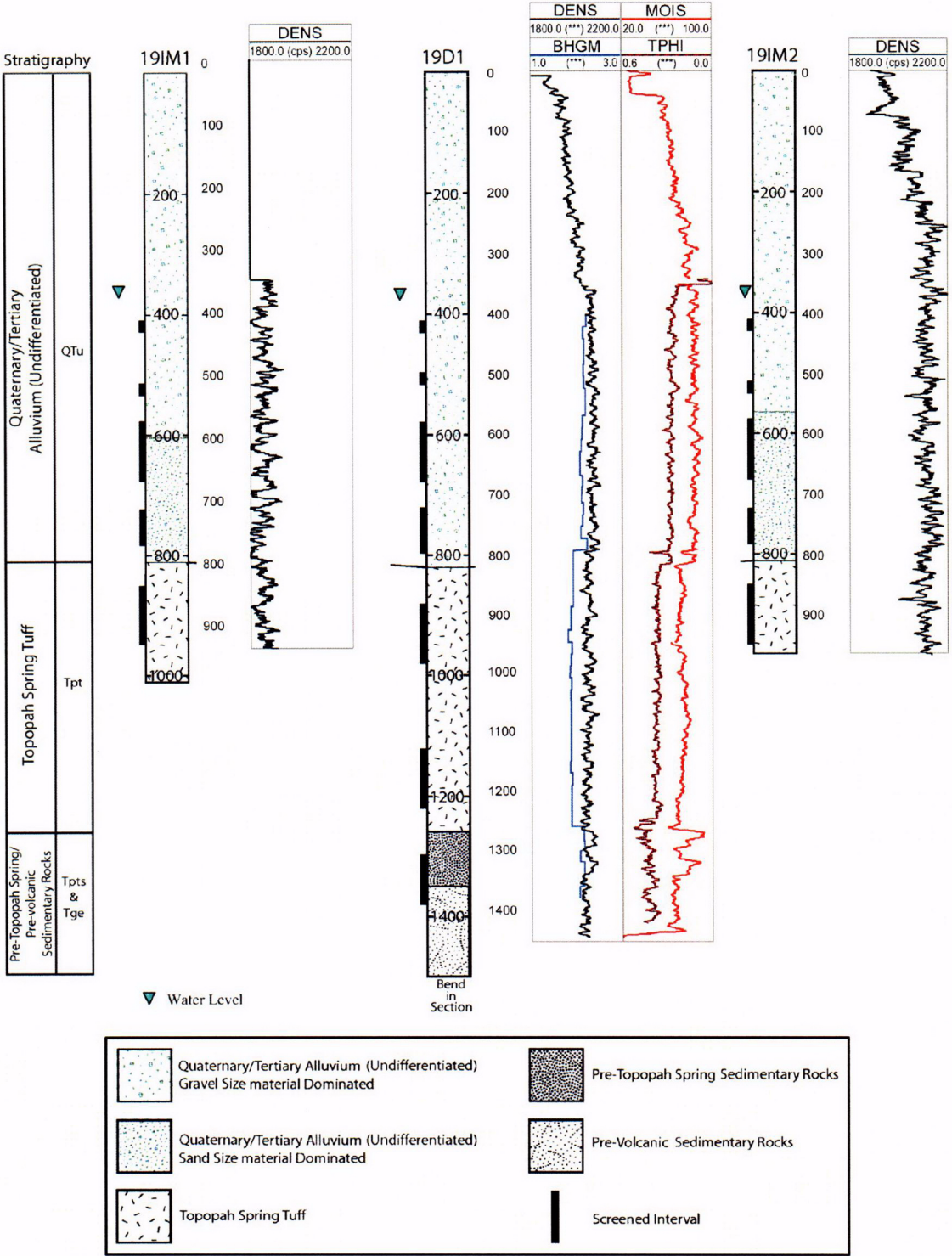
horizontal compressive stress, thus promoting flow in that direction, suggesting a tendency toward dilation and potentially higher permeability (Ferrill et al. 1999, pp. 5 to 6).

Evaluation of the long-term pumping tests at the C-Wells complex supports the conclusion that large-scale horizontal anisotropy of aquifer permeability may occur in the saturated zone. Results of this hydrologic evaluation (Appendix E) generally are consistent with the structural analysis of potential anisotropy and indicate anisotropy that is oriented in a north-northeast to south-southwest direction, assuming the response in borehole USW H-4 is not considered. The response in borehole USW H-4 is consistent with the effect of the Antler Wash fault being superimposed on this uniform anisotropy, resulting in a northwest to southeast anisotropy.

2.3.5.4 Hydrogeologic Characteristics of the Alluvium Derived from Nye County Testing

Hydraulic testing of the alluvium has been performed at the Alluvial Testing Complex (Figure 2-26). Figure 2-30 presents a summary of the lithology in the boreholes at the Alluvial Testing Complex.

One of the most important results from the Alluvial Testing Complex was the interpretation of the “huff-puff” injection-withdrawal tracer test. In this test, a tracer was added to the wellbore and briefly injected into the aquifer. After a period of time (ranging from 0.5 days to 30 days), the tracer was pumped back. The migration of the tracer during the intervening time is controlled by the natural groundwater flux. The results of this test are illustrated in Figure 2-31. Although uncertainty exists in the interpretation of such tests, using reasonable ranges of effective porosity (ranging between 5 and 30 percent), a range of specific discharges in the vicinity of the borehole can be determined. Table 2-7 presents the results of this analysis and indicates a specific discharge in the range of 1.2 to 9.4 m/year.



Source: Location of screened intervals from Questa Engineering Corporation 2002. Lithostratigraphic logs from Spengler 2001b; Spengler 2003a; Spengler 2003b. Borehole names refer to Nye County EWDP boreholes.

Figure 2-30. Summary of Lithology at the Alluvial Testing Complex

Table 2-7. Specific Discharges and Seepage Velocities Estimated from the Different Drift Analysis Methods as a Function of Assumed Flow Porosity

Assumed Flow Porosity ^a	Specific Discharge (m/year) / Seepage Velocity (m/year)		
	0.05	0.18	0.3
Peak Arrival Analysis	1.2 / 24.5	2.4 / 13.1	3.0 / 9.9
Late Arrival Analysis ^b	3.9 / 77.1	7.3 / 40.4	9.4 / 31.3
Mean Arrival Analysis ^c	2.0 / 40.3	3.8 / 20.9	4.9 / 16.4
Mean Arrival Analysis ^d	2.5 / 49.1	4.6 / 25.8	6.0 / 20.2
Linked Analytical Solutions	1.5 / 15 with a flow porosity of 0.10 and a longitudinal dispersivity of 5 m.		

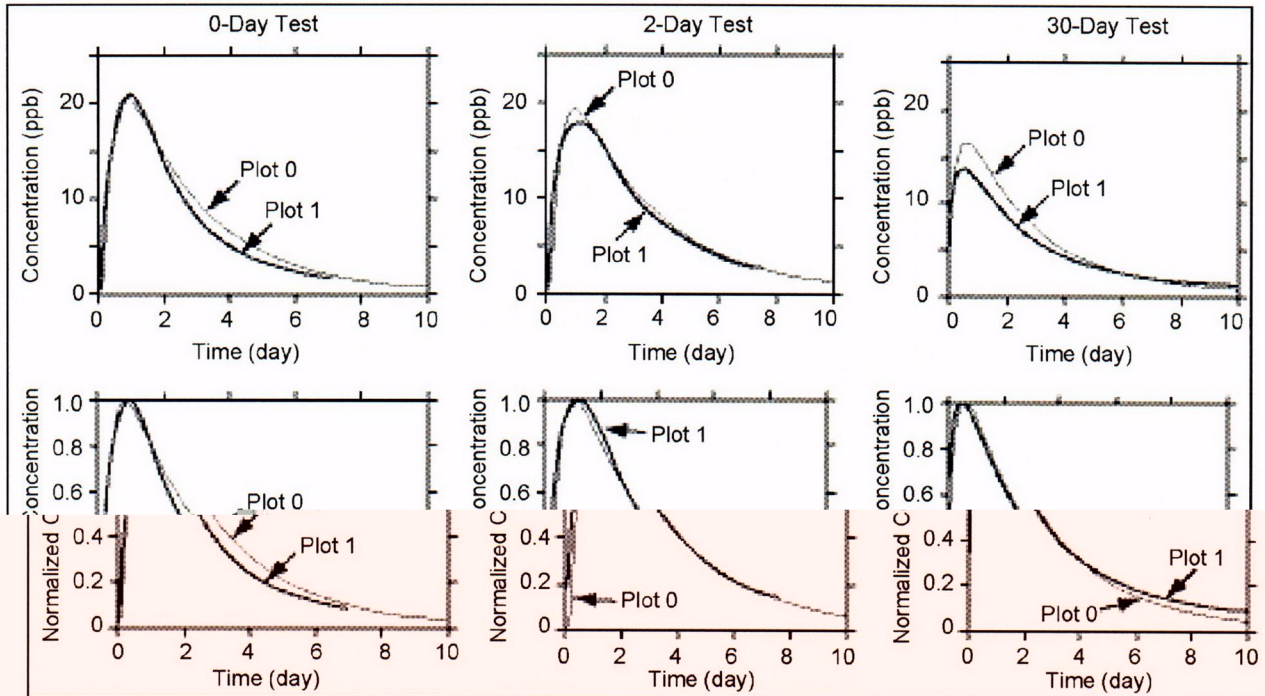
Source: BSC 2003e, Table 6.5-7.

NOTE: ^aThe three values are approximately the lowest, expected, and highest values, respectively, of the alluvium flow porosity used in Yucca Mountain performance assessments (BSC 2001c).

^bTime/Volume associated with approximately 86.4 percent recovery in each test (the final recovery in the 0.5-hr rest period test, which had the lowest final recovery of any test).

^cMean arrival time calculated by truncating all tracer response curves at approximately 86.4 percent recovery in each test.

^dAlternative mean arrival time calculated by extrapolating the tracer response curves in the 0.5-hr rest period test to 91.3 percent and truncating the response curves in the two-day rest period test to 91.3 percent recovery (the final recovery in the 30-day rest period test).



00346DC_091.ai

Source: BSC 2003e, Figure 6.5-26.

NOTE: The plots are fits of three injection-pumpback tracer tests with theoretical curves resulting from three solutions to the advection-dispersion equation for the three phases of injection, drift, and pumpback. "Plot 0" is the model fit and "Plot 1" is the data curve. The parameters used in the calculations are: flow porosity = 0.1; matrix porosity = 0.0; longitudinal dispersivity = 5.05 m; transverse dispersivity = 1.00 m; test interval thickness = 32.0 ft; tracer volume injected = 2,800 gal; chase volume injected = 22,000 gal; injection rate = 15.0 gpm; mass injected = 5.0 kg; natural gradient = 0.002 m/m; T for gradient = 20.0 m^2/day ; specific discharge = 1.5 m/year. The Q values for the 0-, 2-, and 30-day tests are 13.41, 11.00, and 13.50, respectively.

Figure 2-31. Fitting the Injection-Pumpback Tracer Tests in Screen #1 of NC-EWDP-19D1 Using the Linked-Analytical Solutions Method

2.3.6 Site-Scale Geochemistry: Analyses of Water Types and Mixing

Hydrochemical data provide information on several important site-scale issues, including the existence and magnitude of local recharge, flow directions from the repository to downgradient locations, and the potential for mixing and dilution of groundwater that could be released from the repository.

A comparison of hydrochemical and isotopic data from perched water at Yucca Mountain to data from the regional groundwater system suggests that local recharge is a component of the saturated zone waters in volcanic aquifers beneath Yucca Mountain. The data examined included uranium isotopes ($^{234}U/^{238}U$) (Figure 2-32) and major anions and cations. It is possible that shallow groundwater beneath Yucca Mountain is composed entirely of local recharge. For example, by comparing the isotopic signature of perched waters in boreholes USW UZ-14 and USW WT-24 with saturated zone groundwater obtained from boreholes to the southeast, it is apparent that these waters have a similar origin, predominately from vertical recharge through the unsaturated tuff units in the vicinity of Yucca Mountain (BSC 2003f, Section 6.7.6.6).

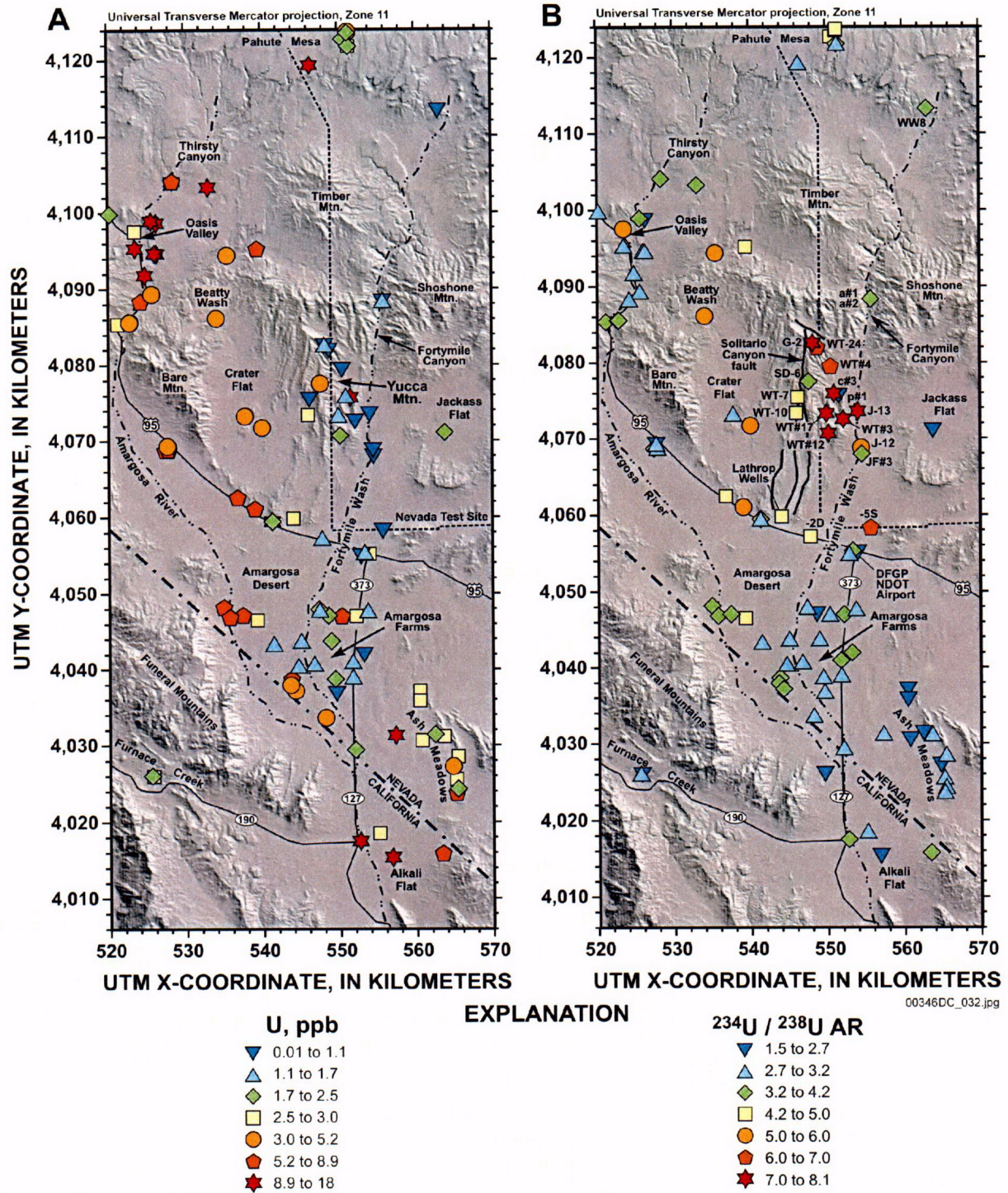


Figure 2-32. Groundwater Uranium and $^{234}\text{U}/^{238}\text{U}$ Ratios in the Vicinity of Yucca Mountain

The chloride concentrations of the groundwater identified from uranium isotopes as having originated from Yucca Mountain have been used to estimate the recharge flux through Yucca Mountain (BSC 2003f, Section 6.7.6.6). Based on the chloride data, and assuming that the chloride flux from precipitation was between one and two times its estimated present-day value, past infiltration rates ranged between 6.5 and 16.5 mm/year. These groundwaters probably infiltrated during the late Pleistocene when the climate was cooler and wetter, so the relatively high infiltration rates should be interpreted as reflecting past, rather than present-day, conditions.

Despite the sometimes large distances between boreholes, differences in regional groundwater chemical and isotopic compositions are often large enough that groundwater flow paths at a regional scale can be identified with some confidence (Figure 2-10). In contrast, despite the closer borehole spacing, the compositions of groundwaters in the immediate vicinity of Yucca Mountain are often too similar to allow detailed flow paths from the repository to be identified with certainty. However, because flow paths do not cross in plan view, possible flow directions from the repository area are constrained by regional Flow Paths 6 and 2 to be dominantly south or southeastward from the repository area. Geochemical inverse models (BSC 2003f, Section 6.7.8) for borehole NC-EWDP-19D indicated that groundwater at this borehole could have originated from the area of borehole UE-25 WT#3 at the mouth of Dune Wash (as depicted by Flow Path 7), or as a result of the mixing of groundwater flowing from the vicinity of borehole USW WT-10 and local Yucca Mountain recharge (indicated schematically by small eastward-pointing arrows on Flow Path 6; Figure 2-10). An origin for NC-EWDP-19D groundwater from the Solitario Canyon area would imply groundwater from the repository area should be forced to flow southeastward toward Fortymile Wash; conversely, an origin for borehole NC-EWDP-19D groundwater from the Dune Wash area near borehole UE-25 WT#3 implies that groundwater from the repository area flows along a more southerly trajectory.

2.3.7 Site Scale Groundwater Flow Model and Results

2.3.7.1 Site-Scale Groundwater Flow Model Development

Development of the site-scale groundwater flow model requires the generation of a computational grid, the identification of the hydrogeologic unit at each node on the grid, the specification of boundary conditions, the specification of recharge values, and the assignment of nodal hydrogeologic properties. Each of these elements of model development is discussed in this section.

The computational grid developed for the site-scale saturated zone flow and transport model was formulated so that the horizontal grid is coincident with the grid cells in the regional-scale flow model. The depth of the computational grid is approximately the same as the depth of the regional-scale saturated zone flow model. The computational grid begins at the water table surface and extends to a depth of 2,750 m below sea level.

The vertical grid spacing was established to provide the resolution necessary to represent flow and transport along critical flow and transport pathways in the saturated zone. A finer grid spacing was adopted for shallower portions of the model, while a progressively coarser grid was adopted for deeper portions of the aquifer. The vertical grid spacing ranged from 10 m near the water table to 550 m at the bottom of the model domain. The vertical dimension of the model

2.3.7.2 Site-Scale Groundwater Flow Model Comparisons to Observations

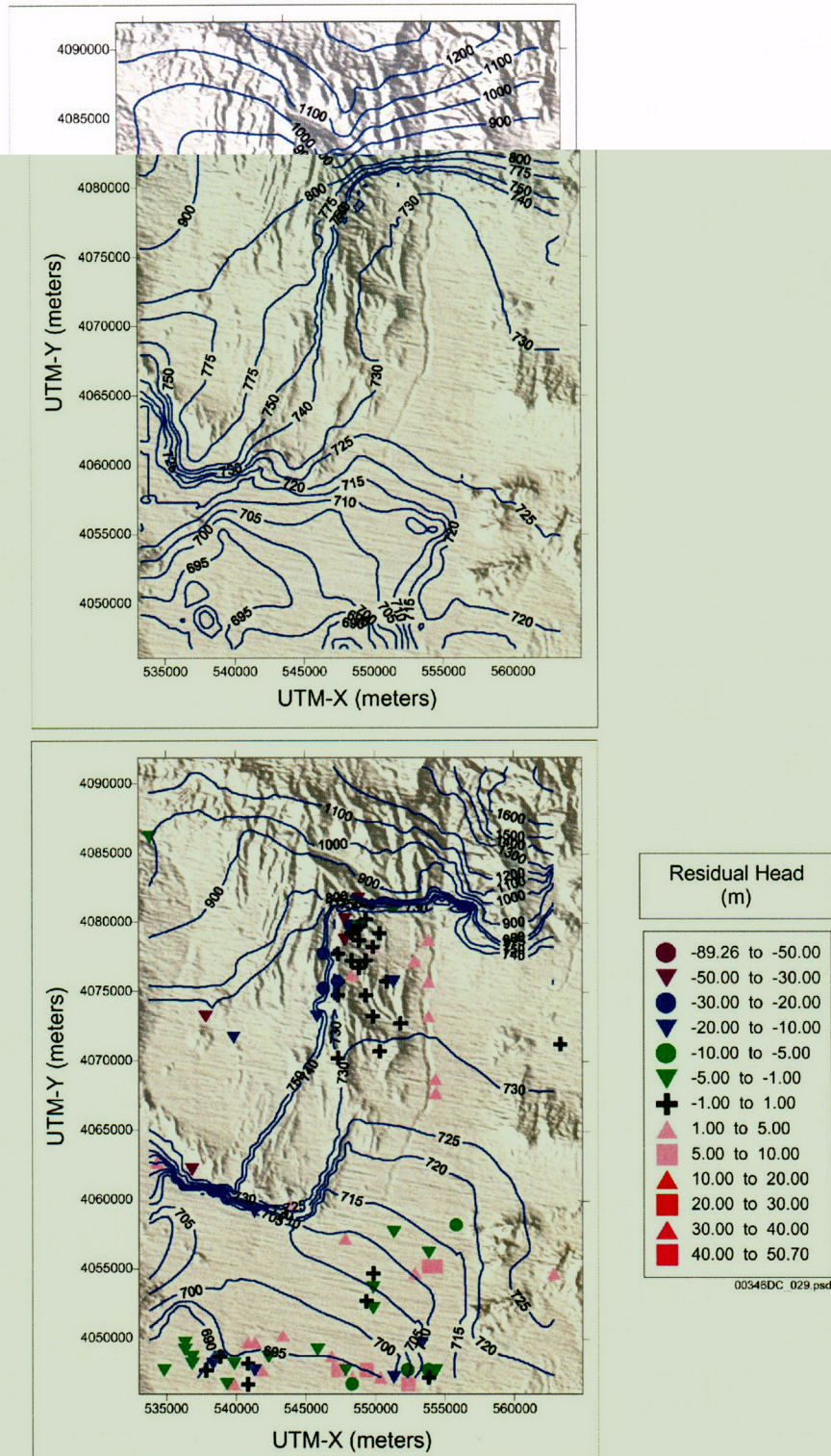
The results of the calibrated site-scale saturated zone flow and transport model have been compared to direct and indirect indicators of groundwater flow processes. These analyses include a comparison between: (1) the observed and predicted water-level data, (2) calibrated and observed permeability data, (3) boundary fluxes predicted by the regional-scale flow model and the calibrated site-scale saturated zone flow model, (4) the observed and predicted gradients between the carbonate aquifer and overlying volcanic aquifers, (5) hydrochemical data and particle pathways predicted by the model, and (6) thermal data.

Predicted and Observed Water-Level Elevations—Predicted and observed heads from the site-scale groundwater flow model are illustrated in Figure 2-34. As in the case of the regional model, the comparison is favorable in areas of low hydraulic gradient, but becomes more uncertain in areas of steep gradients. In the areas downgradient from Yucca Mountain, the match is acceptable.

Since the site-scale flow model was calibrated, a number of boreholes have been installed as part of the Nye County Early Warning Drilling Program. These new boreholes include those installed at new locations and those completed at depths different from those previously available at existing locations. Comparison of water levels observed in the new Nye County Early Warning Drilling Program boreholes with water levels predicted by the calibrated site-scale flow model at these new locations and depths offered an opportunity to validate the site-scale flow model using new data not used for developing and calibrating the flow model. Predicted and observed water levels are provided in Table 2-8.

Examination of the residuals (Table 2-8) indicates that uncertainty associated with the predicted water levels depends on the location of the borehole within the site-scale model domain. Residuals generally are higher in the western portion of the Nye County Early Warning Drilling Program area. The gradients are steeper in this area, and the calibrated model generally is less capable of predicting these steeper gradients.

The observed residuals tend to improve at boreholes located further to the east. For example, residuals in the general area of NC-Washburn-1X, NC-EWDP-4, and NC-EWDP-5 are low. These boreholes are in the flow path inferred by hydrochemical data, and therefore these additional water-level data support the capability of the site-scale flow model to predict water levels in this portion of the flow path.



Source: Based on BSC 2003c, Figures 6.4-5 and 6.4-6.

NOTE: Upper figure represents observed hydraulic heads; lower figure represents predicted hydraulic heads and head residuals (predicted minus observed heads).

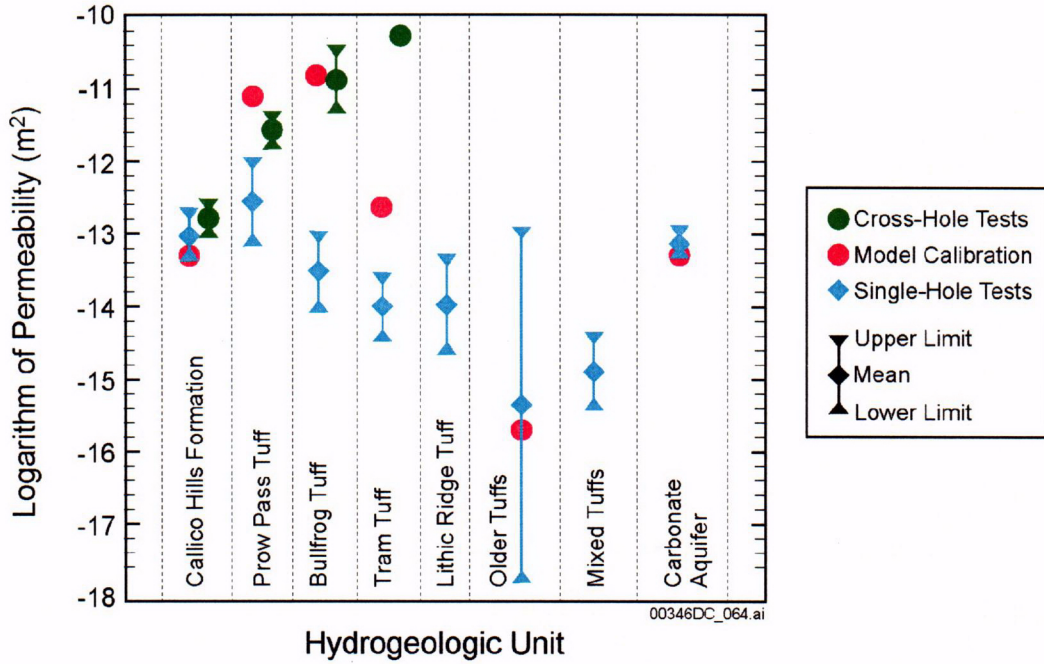
Figure 2-34. Comparison of Observed and Predicted Hydraulic Heads in the Site-Scale Groundwater Flow Model

Table 2-8. Comparison of Observed and Predicted Water Levels at Nye County Early Warning Drilling Program Boreholes

Site Name	x (m)	y (m)	Observed Head (m)	Modeled Head (m)	Residual Error (m)
NC-EWDP-1DX, deep	536768	4062502	748.8	762.7	13.9
NC-EWDP-1DX, shallow	536768	4062502	786.8	756.7	-30.1
NC-EWDP-1S, P1	536771	4062498	787.1	767.3	-19.8
NC-EWDP-1S, P2	536771	4062498	786.8	767.3	-19.5
NC-EWDP-2DB	547800	4057195	713.7	717.0	4.3
NC-EWDP-2D	547744	4057164	706.1	709.2	3.3
NC-EWDP-3D	541273	4059444	718.3	703.7	-14.6
NC-EWDP-3S, P2	541269	4059445	719.8	702.5	-17.3
NC-EWDP-3S, P3	541269	4059445	719.4	702.6	-16.8
NC-EWDP-5SB	555676	4058229	723.6	718.0	-6.6
NC-EWDP-9SX, P1	539039	4061004	766.7	731.7	-35.0
NC-EWDP-9SX, P2	539039	4061004	767.3	731.7	-35.6
NC-EWDP-9SX, P4	539039	4061004	766.8	731.7	-35.1
NC-Washburn-1X	551465	4057563	714.6	714.5	-0.1
NC-EWDP-4PA	553167	4056766	717.9	715.5	-2.4
NC-EWDP-4PB	553167	4056766	723.6	715.5	-8.1
NC-EWDP-7S — Zone 1	539638	4064323	818.1	769.6	-48.5
NC-EWDP-7S — Zone 2	539638	4064323	786.4	769.6	-16.8
NC-EWDP-7S — Zone 3	539638	4064323	756.6	769.6	13.0
NC-EWDP-7S — Zone 4	539638	4064323	740.2	769.6	29.4
NC-EWDP-12PA	536951	4060814	722.9	705.3	-17.6
NC-EWDP-12PB	536951	4060814	723.0	705.3	-17.7
NC-EWDP-12PC	536951	4060814	720.7	704.3	-16.4
NC-EWDP-15P	544848	4058158	722.5	711.0	-11.5
NC-EWDP-19P	549329	4058292	707.5	713.2	5.7
NC-EWDP-19D	549317	4058270	712.8	713.2	0.4
NC-EWDP-16P	545648	4064247	730.9	711.0	-19.9
NC-EWDP-27P	544936	4065266	730.3	713.2	-17.1
NC-EWDP-28P	545723	4062372	729.7	713.2	-16.5

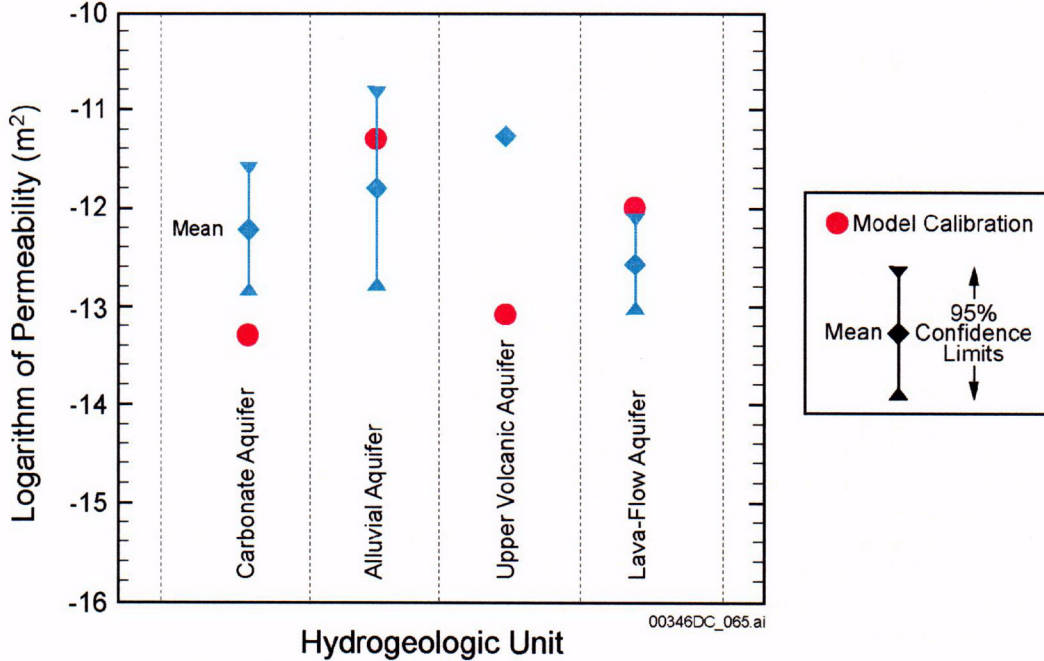
Source: BSC 2003c, Table 7.1-2.

Permeability—For model validation, the permeabilities estimated during calibration of the site-scale saturated zone flow and transport model were compared to permeabilities determined from aquifer test data from the Yucca Mountain area and elsewhere at the Nevada Test Site (BSC 2003c, Section 7). The logarithms of permeability estimated during calibration of the model were compared to the mean logarithms of permeability determined from aquifer test data from Yucca Mountain (Figure 2-35) and to data from elsewhere at the Nevada Test Site (Figure 2-36). For most geologic units, calibrated permeabilities were within the 95 percent confidence limits of the mean permeabilities estimated from the data. Given the available data, the agreement between the model-calibrated value and the estimated site permeability value for the carbonate aquifer is considered to provide an adequate basis for confidence in the validity and representativeness of the site-scale flow model.



Source: Based on BSC 2001a, Figure 14.

Figure 2-35. Comparison of Calibrated and Observed Permeabilities from Yucca Mountain Pump Test Data in the Site-Scale Groundwater Flow Model



Source: BSC 2001a, Figure 15.

Figure 2-36. Comparison of Calibrated and Observed Permeabilities from Nevada Test Site Pump Test Data in the Site-Scale Groundwater Flow Model

C14

With the exception of the calibrated values for the upper volcanic aquifer, the calibrated permeabilities generally are consistent with most of the permeability data from Yucca Mountain and elsewhere at the Nevada Test Site. A discrepancy exists between the calibrated permeability for the Tram Tuff and the mean permeability derived from the cross-hole tests. However, permeabilities measured for the Tram Tuff of the Crater Flat Group may have been enhanced by the presence of a breccia zone in the unit at boreholes UE-25 c#2 and UE-25 c#3 (Geldon et al. 1997, Figure 3; BSC 2003e).

The permeability data obtained from single-hole and cross-hole testing at the Alluvial Testing Complex also compare acceptably with the permeabilities predicted in the site-scale flow model. Single-well hydraulic testing of the saturated alluvium in borehole NC-EWDP-19D1 was conducted between July 2000 and November 2000. During this testing, a single-well test of the alluvial aquifer to a depth of 247.5 m below land surface at the NC-EWDP-19D1 resulted in a permeability measurement of $2.7 \times 10^{-13} \text{ m}^2$ (BSC 2003c; Table 7.2-1). A cross-hole hydraulic test was also conducted at the Alluvial Testing Complex in January 2002. During this test, borehole NC-EWDP-19D1 was pumped in the open-alluvium section, while water-level measurements were made in the two adjacent boreholes. The intrinsic permeability measured in this test for the tested interval is $2.7 \times 10^{-12} \text{ m}^2$. The calibrated permeability for the Alluvial Uncertainty Zone was $3.2 \times 10^{-12} \text{ m}^2$. Because the cross-hole tests intercepted a larger volume of rock, they are considered to be more representative of the water-transmitting capability at this location, and therefore they are more appropriate for comparison with the calibrated permeability values.

Boundary Fluxes—A comparison of fluxes at the boundary of the site-scale model domain predicted by the regional-scale model and the calibrated site-scale saturated zone flow and transport model was used to further validate the site-scale model (CRWMS M&O 2000a, Section 3.4.2). Volumetric fluxes computed along the boundary by the two models match acceptably well (Table 2-4). The total fluxes across the northern boundary computed by the regional and site-scale models were $6.0 \times 10^6 \text{ m}^3/\text{year}$ and $5.3 \times 10^6 \text{ m}^3/\text{year}$, respectively. The boundary fluxes computed along the east side of the site-scale saturated zone flow model domain also indicate a good match. The total fluxes across the eastern boundary computed by the regional and site-scale models were 1.8×10^7 and $1.6 \times 10^7 \text{ m}^3/\text{year}$, respectively. The match is particularly good along the lower thrust area where both models predict large fluxes across the boundary. Both models also predicted small fluxes across the remainder of the eastern boundary. The effect of the small differences between the two flux predictions on the specific discharge is within the uncertainty range used. The southern boundary flux is simply a sum of the other boundary fluxes plus recharge. Fluxes across the southern boundary computed by the two models indicate a relatively good match. The difference in the fluxes computed by the regional and site-scale models across the southern boundary is approximately 2.9×10^7 and $2.3 \times 10^7 \text{ m}^3/\text{year}$, respectively (Table 2-4).

Upward Hydraulic Gradient—An upward hydraulic gradient between the lower carbonate aquifer and the overlying volcanic rocks has been observed in the vicinity of Yucca Mountain. Principal evidence for this upward gradient is provided by data from boreholes drilled into the upper part of the carbonate aquifer (UE-25 p#1 and NC-EWDP-2DB). Hydraulic head measurements in borehole UE-25 p#1 indicate that the head in the carbonate aquifer is about 752 m, which is about 21 m higher than the head measured in this borehole in the overlying

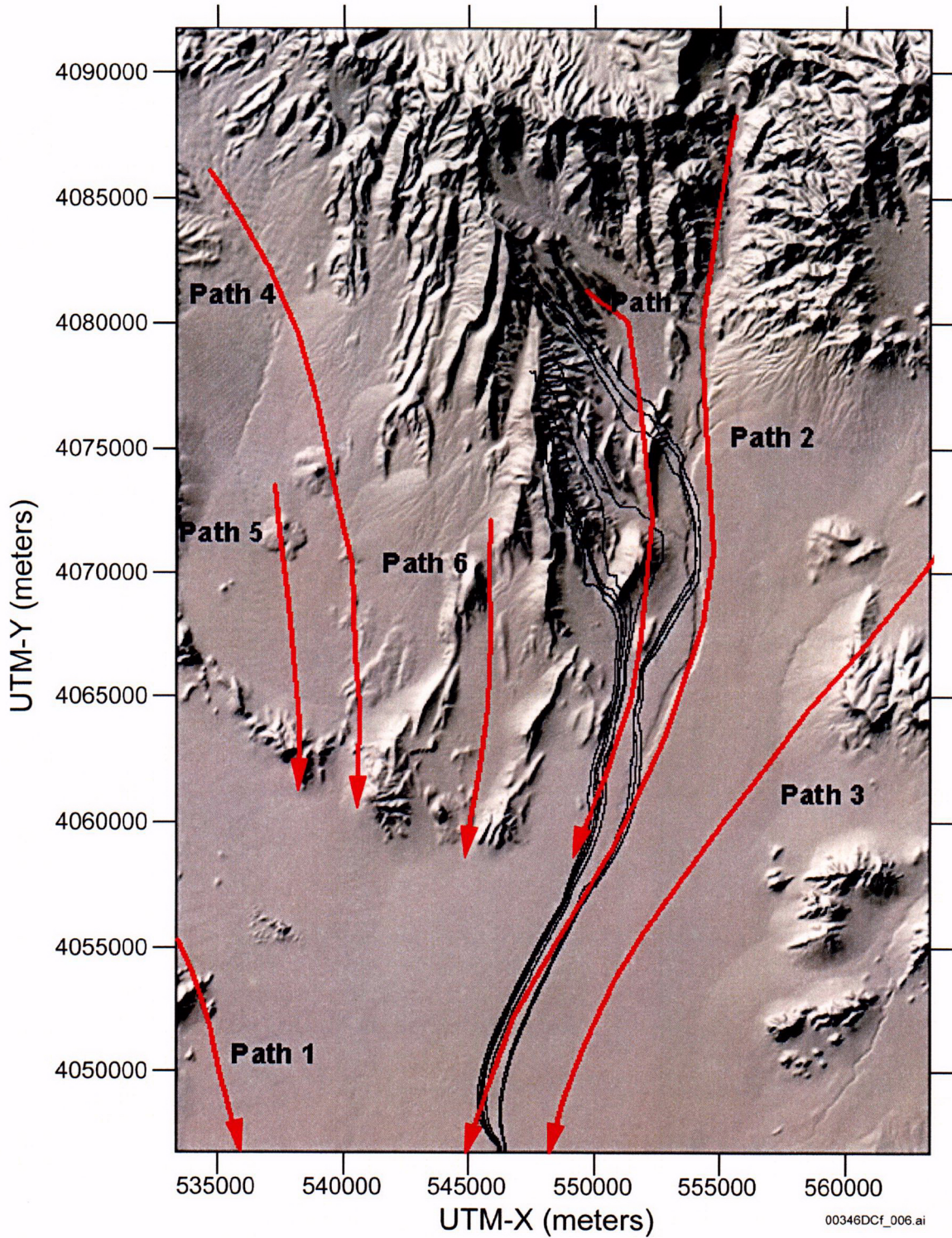
volcanic rocks. The head in the carbonate aquifer at this borehole was estimated as part of the model calibration process. The increasing head with depth was preserved during model calibration, although the head difference was only 12.73 m (BSC 2003c, Table 16). The difference in predicted and observed upward hydraulic gradient values at this location results, in part, because the constant vertical head boundary conditions imposed on the lateral boundaries of the model domain constrained the vertical groundwater flow and gradients within the model interior (CRWMS M&O 2000a, Sections 6.7.11 and 6.1.2).

Hydrochemical Data Trends—To provide further validation of the site-scale saturated zone flow and transport model, flow paths (Figure 2-37) predicted by the calibrated model were compared with those estimated using groundwater chemical and isotopic data (Figure 2-10). Flow paths predicted by the calibrated site-scale saturated zone flow model were generated using the particle-tracking capability of the Finite Element Heat and Mass Transfer Code (Zyvoloski et al. 1997) by placing particles at different locations beneath the repository and running the model to trace the paths of these particles across a range of horizontal anisotropies.

Comparison of the flow paths indicate that most of the particles travel between Flow Paths 2 and 6, and they roughly follow the trajectory of Flow Path 2 through the alluvium along the west side of Fortymile Wash. These particle trajectories are permitted by the constraints provided by the groundwater geochemical and isotopic data.

Thermal Modeling—Temperature measurements can be used as an indirect indicator of groundwater flow. Although uncertainty exists in the interpretation of the thermal anomalies in that they could result from thermal properties (notably thermal conductivity), heat flux, or overburden variability, and not the result of areal or vertical groundwater flux, an acceptable comparison of observed and simulated temperatures for the site-scale flow model has been obtained. The temperature data used in the thermal modeling are taken from temperature profiles measured within the model domain. The temperature data were extracted at 200-m intervals from these temperature profiles, and a total of 94 observations from 35 boreholes were obtained.

Coupled thermal modeling and conduction-only modeling have been completed to evaluate the consistency of the saturated zone flow model with the thermal observations. The details related to this thermal modeling are presented in Appendix D. Given the uncertainties associated with interpreting the thermal anomalies, the results presented in Appendix D provide a reasonable comparison.



Source: BSC 2003c, Figure 7.3-1b.

NOTE: Black lines are predicted flow paths; red lines with arrowhead are flow paths inferred from geochemical data (Figure 2-11)

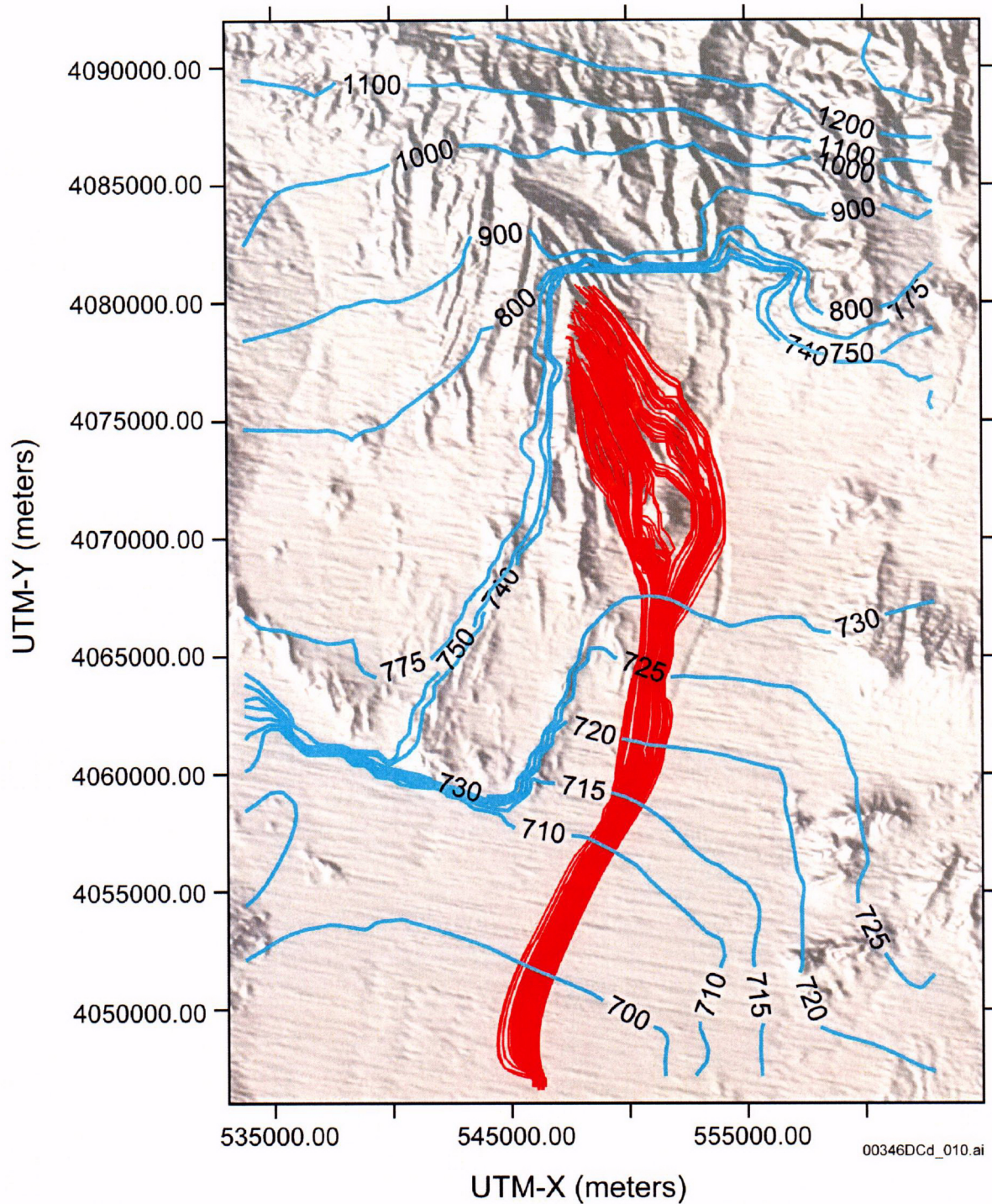
Figure 2-37. Predicted Groundwater Flow Path Trajectories and Flow Paths Inferred from Geochemistry

2.3.7.3 Model Results

Using the calibrated flow model, specific discharge was estimated for a nominal fluid path leaving the repository area and traveling 0 to 5 km, 5 to 20 km, and 20 to 30 km. The specific discharge simulated by the flow model for each segment of the flow path was determined using the median travel time for a group of particles released beneath the repository. Specific discharge values of 0.67, 2.3, and 2.5 m/year were obtained for the three flow path segments, respectively. The first segment reflects flow in the tuff aquifers, and the last segment reflects flow in the alluvial aquifer. An expert elicitation panel was convened prior to the site recommendation (CRWMS M&O 1998, Figure 3-2e), and it estimated a specific discharge of 0.71 m/year for the 0-to-5-km segment. Thus, the specific discharge values predicted by the model and the expert elicitation panel were similar. In addition, the lower end of the range of inferred specific discharges from the single-well tracer-injection test conducted in the alluvial aquifer (1.2 and 9.4 m/year) acceptably reproduces the median-modeled specific discharge at this location (about 2.3 m/year).

The particle-tracking capability of the Finite Element Heat and Mass Transfer Code (Zyvoloski et al. 1997) was used to illustrate flow paths predicted by the calibrated site-scale saturated zone flow and transport model. One hundred particles were distributed uniformly over the area of the repository and allowed to migrate until they reached the model boundary (Figure 2-38). The pathways leave the repository and generally travel south-southeasterly to the 18-km compliance boundary.

The flow paths from the water table beneath the repository to the accessible environment directly affect breakthrough curves and associated radionuclide travel times. Because the flow paths and water table transition from volcanic tuffs to alluvium, flow path uncertainty directly affects the length of flow in the volcanic tuffs and in the alluvium. Uncertainty in flow paths is affected by permeability anisotropy of the volcanic tuffs. Large-scale anisotropy and heterogeneity were implemented in the saturated zone site-scale flow model through direct incorporation of known hydraulic features, faults, and fractures. Detailed discussion of the uncertainty in flow path lengths in the tuff aquifers prior to intersecting the alluvial aquifers is presented in Appendix G.



Source: Based on BSC 2003c, Figure 6.6-3.

Figure 2-38. Predicted Saturated Zone Particle Trajectories from Yucca Mountain

2.4 SUMMARY

The regional and site-scale groundwater flow representations indicate that groundwater in the shallow tuff aquifers flows south-southeasterly from the repository and parallels Fortymile Wash to the point where it discharges from the shallow tuff aquifers and mixes with other groundwater in the alluvium of the Amargosa Desert. The flow paths are acceptably constrained by the available hydrogeologic and geochemical information, and the location of the tuff-alluvium contact is also acceptably constrained by recent drilling and geophysics conducted by Nye County. The exact location where groundwater at the water-table enters the alluvium is uncertain. This uncertainty is due, in part, to uncertainty in the flow paths, which is due to uncertainty in anisotropy and in the tuff-alluvium contact. The uncertainty in the tuff-alluvium contact is included in the uncertainty of radionuclide transport times along the likely paths of radionuclide migration in the saturated zone.

The average flow rate in the alluvium, as defined by the specific discharge distribution in the alluvium, has been independently evaluated to be about 2.5 m/year, with a range of about 1.2 to 9.4 m/year. To account for uncertainty in the hydraulic properties and specific discharge, a range of specific discharge values was used in the assessment of repository performance. The values ranged from a factor of one-third to a factor of three times the median specific discharge.

The regional and site-scale groundwater flow models have been calibrated with potentiometric, recharge, discharge, and hydraulic characteristic observations. In addition, these flow models have been independently corroborated with geochemical observations (conservative tracers and stable isotopes), thermal observations, and tracer test determinations of specific discharge.

INTENTIONALLY LEFT BLANK